

Reduction and reorientation of Cr magnetic moments in Fe/Cr multilayers observed by a ^{119}Sn Mössbauer probe

M. Almokhtar,* K. Mibu, and T. Shinjo

Institute for Chemical Research, Kyoto University, Uji, Kyoto-fu 611-0011, Japan

(Received 14 January 2002; revised manuscript received 16 May 2002; published 2 October 2002)

The magnetism of Cr thin films in Fe/Cr multilayers was studied using ^{119}Sn subatomic layers inserted in the Cr layers as a Mössbauer probe for Cr layer thickness from 10 to 160 Å. The size and direction of the Cr magnetic moments were inferred from the size and direction of the magnetic hyperfine fields at the Sn nuclear sites. The detected magnetic hyperfine fields indicate that the Cr magnetic moments reduce as the Cr layer thickness decreases, while they do not remarkably change as a function of the distance from the Fe/Cr interface. The magnetic hyperfine fields for the samples grown at 200 °C are smaller and more oriented to the film plane than for the samples grown at room temperature. These observations suggest that the magnetic frustration resulting from Fe/Cr interface imperfections is accommodated by the reduction of the Cr magnetic moments for the samples grown at elevated temperatures, whereas it is accommodated by the reorientation of Cr magnetic moments toward the perpendicular direction to the Fe magnetic moments for the samples grown at lower temperatures.

DOI: 10.1103/PhysRevB.66.134401

PACS number(s): 75.70.-i, 75.25.+z, 76.80.+y

I. INTRODUCTION

In Fe/Cr multilayers, the interplay between the Fe-Cr interlayer coupling at the interfaces and the magnetic order of Cr layers is a matter of intensive discussion.^{1,2} Bulk Cr orders below the Néel temperature $T_N=311$ K as an incommensurate spin-density wave with a sinusoidal modulation of the magnetic moments.³ In Fe/Cr(001) multilayers with ideally flat interfaces, the energy minimum is satisfied by the Fe-Cr antiferromagnetic coupling at the Fe/Cr interfaces, the ferromagnetic coupling within the Fe layers, and the Cr-Cr antiferromagnetic coupling within the Cr layers. In real Fe/Cr superlattices, where the Fe/Cr interfaces are not ideally flat, some atomic pairs would not necessarily be in their minimum exchange energy, and therefore cannot keep their preferred alignment. The influence of the interfacial frustration is expected to be contained in the Cr layers rather than in the Fe layers or at the interfaces.^{4,5} One possible way to accommodate the magnetic frustration resulting from the steps at the interfaces is forming domain walls connecting the steps at adjacent interfaces for thin Cr layers, or forming domain walls connecting the steps at the same interface for thick Cr layers.^{4,5} On the other hand, tight-binding calculations predict that the Fe/Cr interfaces with interdiffusion suppress the nearby Cr magnetic moments to reduce the frustrated magnetic coupling energy.^{6,7} In Fe/Cr multilayers with steps at the interfaces, it is also predicted that a noncollinear commensurate spin-density wave (CSDW) exists in the Cr layers, and a noncollinear coupling between Fe layers appears to keep the antiferromagnetic structure in the Cr layer with inhomogeneous layer thickness.⁸⁻¹⁰

Experimentally, neutron-diffraction studies on Fe/Cr superlattices show that Cr layers with thickness larger than 42 Å form a transverse spin-density wave (TSDW) with the Cr magnetic moments lying in the film plane and the wave vector perpendicular to the film plane at low temperatures.¹¹⁻¹⁷ The TSDW minimizes the frustrated magnetic coupling energy at the imperfect Fe/Cr interfaces by shifting its nodes to the interfaces and magnetically decoupling the Cr layers

from the adjacent Fe layers.¹¹ The Fe/Cr multilayers grown by magnetron sputtering on MgO(001) substrates at 100 °C show a transition from TSDW to the paramagnetic state with increasing temperature.¹⁶ On the other hand, the Fe/Cr superlattices grown on Al_2O_3 (1102) substrates at 300 °C by molecular-beam epitaxy (MBE) show that the Cr layer with the thickness of 80 Å has a transition from CSDW to TSDW below 250 K, while the Cr with the thickness of 42 Å has a CSDW down to 30 K.^{14,15} At small Cr thickness, the existence of a spiral CSDW in the Cr of the Fe/Cr multilayers grown on Al_2O_3 (1102) or GaAs(001) substrates at elevated temperatures has been suggested indirectly by detecting a strong noncollinear magnetic coupling between the Fe layers, using the magneto-optic Kerr effect and polarized neutron reflectometry.^{15,17,18} In the case of Fe/Cr multilayers grown at room temperature, a ferromagnetically coupled or uncoupled behavior between the Fe layers was detected and the Cr layers were assumed to be nonmagnetic.¹⁷ Perturbed angular correlation measurements show that the Cr layers in Fe/Cr multilayers grown by MBE on MgO(001) substrates at 150 °C are nonmagnetic below 51 Å. At larger thickness and low temperatures, Cr layers order with a longitudinal spin-density wave while Fe/Cr multilayers grown on Al_2O_3 (1102) substrates at 300 °C order with a TSDW.^{19,20} These distinct differences in the magnetic structure of Cr layers are believed to be correlated with the length scale of the Fe/Cr interface roughness, which in turn depends on the growth conditions.^{1,2} The investigations of Fe/Cr multilayers grown at different temperatures show that samples grown at room temperature were characterized by a small terrace length and a large density of steps at the Fe/Cr interfaces, compared with samples grown at elevated temperatures.¹⁷ Therefore the frustration energy is expected to be larger for the samples grown at room temperature and consequently the effect on the Cr spin order would be stronger.

For a further understanding of the effect of the growth conditions on the Cr magnetization in Fe/Cr multilayers, we investigated the local magnetic structure, such as the magnitude of the magnetic moment and the atomic spin orientation

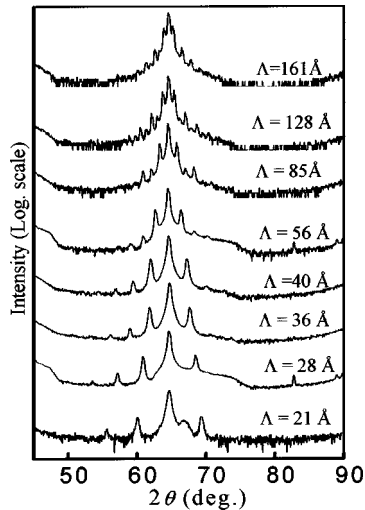


FIG. 1. X-ray diffraction patterns in the high-angle region for $[\text{Fe} (10 \text{ \AA})/\text{Cr} (t \text{ \AA})/\text{Sn} (1 \text{ \AA})/\text{Cr} (t \text{ \AA})]_{\times 29}/\text{Fe} (10 \text{ \AA})$, $2t = 10, 16, 24, 28, 44, 80, 120$, and 160 \AA , grown at 200°C . The estimated multilayer periods are shown.

of Cr, in Fe/Cr multilayers grown on the MgO(001) substrates at 200°C and at room temperature using ^{119}Sn (1 \AA) inserted in the Cr layers as a Mössbauer probe.

II. EXPERIMENTAL PROCEDURE

$[\text{Fe} (10 \text{ \AA})/\text{Cr} (t \text{ \AA})/\text{Sn} (1 \text{ \AA})/\text{Cr} (t \text{ \AA})]_{\times 39}/\text{Fe} (10 \text{ \AA})$ multilayers were epitaxially grown in the bcc [001] direction on MgO(001) at 200°C and at room temperature using an ultrahigh vacuum deposition technique with e -gun heating. A Cr (50 \AA) buffer layer was deposited at 200°C on the MgO(001) substrate prior to the multilayer growth for both growth temperatures in order to relieve the strain resulting from the MgO substrate. The deposition rate was set around 0.3 \AA/s and the pressure was in the 10^{-9} -Torr range. The thickness of the Fe layers was fixed at 10 \AA and the Cr layer thickness between two Fe layers, $t_{\text{Cr}} = 2t$, was changed from 10 to 160 \AA . The crystallographic structure of Cr and Fe layers was checked by x-ray diffraction (XRD) in high- and low-angle regions using Cu $K\alpha$ radiation. The in-plane lattice spacing was investigated through off-axis x-ray diffraction scans around the bcc Cr(112) peak. The current-in-plane magnetoresistance measurements were carried out with a conventional four-point-probe method and with an external magnetic field applied in the film plane parallel to the electric current. The local magnetic properties of the Cr layers at room temperature were probed through ^{119}Sn conversion electron Mössbauer spectroscopy using a $\text{Ca}^{119\text{m}}\text{SnO}_3$ γ -ray source and a He + 1% $(\text{CH}_3)_3\text{CH}$ gas-flow counter. The direction of the incident γ rays was set parallel to the film normal.

III. RESULTS AND DISCUSSION

A. Structural characterization

Bulk Cr and Fe have a similar bcc structure with the lattice constants at room temperature of 2.88 and 2.87 \AA , re-

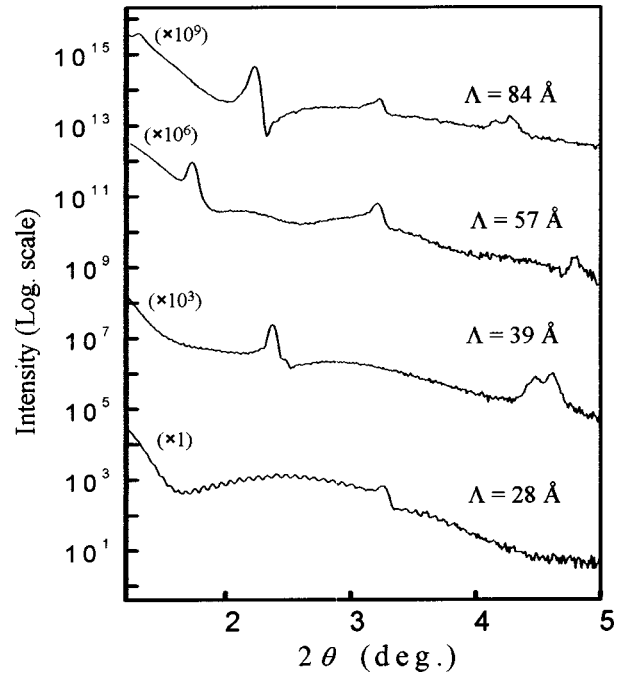


FIG. 2. X-ray diffraction patterns in the low-angle region for $[\text{Fe} (10 \text{ \AA})/\text{Cr} (t \text{ \AA})/\text{Sn} (1 \text{ \AA})/\text{Cr} (t \text{ \AA})]_{\times 29}/\text{Fe} (10 \text{ \AA})$, $2t = 16, 28, 44$, and 80 \AA , grown at 200°C . The estimated multilayer periods are shown. The intensity is multiplied by the value shown above each curve on the left side to shift the base line up in the y axis.

spectively. The high-angle XRD measurements in the θ - 2θ scan with the scattering vector normal to the film plane for the samples grown at 200°C are shown in Fig. 1. The observation of the Fe/Cr/Sn/Cr(002) fundamental peak with superlattice satellite peaks indicates that Fe and Cr grow epitaxially with the [001] direction perpendicular to the film plane, and that the artificial periodicity is well established through the samples. Sn was found to grow epitaxially with Cr and the Sn atoms are expected to locate on the substitutional sites of the bcc Cr(001) lattice, forming a little strained bcc lattice with the Cr atoms.²¹ The modulation periods were estimated from the positions of satellite peaks using the relation $\Lambda = 2\pi/\delta Q$, where δQ is the average spacing between the Q values of the peaks ($Q = 4\pi \sin \theta/\lambda$), and agree well with the designed period as shown in Fig. 1. The high-angle x-ray diffraction patterns for multilayers grown at room temperature show also good epitaxial growth.

The low-angle x-ray patterns for the samples grown at 200°C and at room temperature are shown in Figs. 2 and 3 for comparison. The periods determined from the peak positions agree with the values obtained from the high-angle diffraction patterns. The feature of the diffraction patterns indicates that the layers have well-defined interfaces for both growth temperatures. The samples grown at 200°C appear to have sharper interfaces than those grown at room temperature as inferred from the decay of the intensity of the higher-order Bragg peaks as a function of the scattering vector. This result agrees well with the x-ray diffraction studies for Fe/Cr superlattices without Sn, which also show that the interfacial roughness is generally larger for the samples grown at room

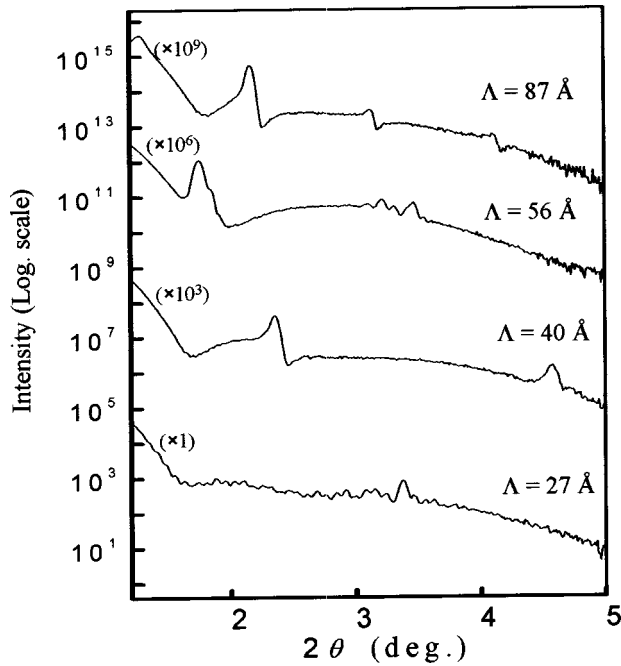


FIG. 3. X-ray diffraction patterns in the low-angle region for $[\text{Fe}(10 \text{ \AA})/\text{Cr}(t \text{ \AA})/\text{Sn}(1 \text{ \AA})/\text{Cr}(t \text{ \AA})]_{\times 29}/\text{Fe}(10 \text{ \AA})$, $2t=16, 28, 44,$ and 80 \AA , grown at room temperature. The estimated multilayer periods are shown. The intensity is multiplied by the value shown above each curve on the left side to shift the base line up in the y axis.

temperature than those grown at higher temperatures.^{1,2,17,18} Note that the surface mobility reduces by decreasing the growth temperature and therefore lower substrate temperatures introduce more steps in the superlattice.²² The structural properties of Fe/Cr superlattices with submonatomic Sn layers inserted in the Cr layers, where four different interfaces (i.e., Fe/Cr, Cr/Sn, Sn/Cr, and Cr/Fe) exist, have been quantitatively examined by x-ray reflectivity and diffuse scattering measurements using synchrotron radiation near the Fe and Cr absorption edge.²³ It is shown that the roughness structure is not much different for the four kinds of interfaces and the Sn atoms form ultrathin layers rather than being dispersed in the Cr layers, and that the estimated root-mean-square roughness is around 6 \AA for the Fe/Cr multilayers with the Sn probe grown at 200°C .

The x-ray diffraction measurements with the scattering vector in the film plane show that the structural relation in the film plane is $\text{MgO}[100]/\text{Cr}[110]/\text{Fe}[110]$. The estimated in-plane (100) lattice constant for $[\text{Fe}(10 \text{ \AA})/\text{Cr}(5 \text{ \AA})/\text{Sn}(1 \text{ \AA})/\text{Cr}(5 \text{ \AA})]_{\times 39}/\text{Fe}(10 \text{ \AA})$ is 2.89 \AA , indicating that the average in-plane unit-cell dimensions do not remarkably change by inserting the Sn probe.

B. Magnetoresistance measurements

Magnetoresistance measurements at 300 K for the samples designated as $[\text{Fe}(10 \text{ \AA})/\text{Cr}(t \text{ \AA})/\text{Sn}(1 \text{ \AA})/\text{Cr}(t \text{ \AA})]_{\times 39}/\text{Fe}(10 \text{ \AA})$, where the Cr thickness $t_{\text{Cr}}=2t=10, 16,$ and 24 \AA are shown in Fig. 4. The saturation field decreases from 1 to 0.15 T and increases again to 0.3 T when

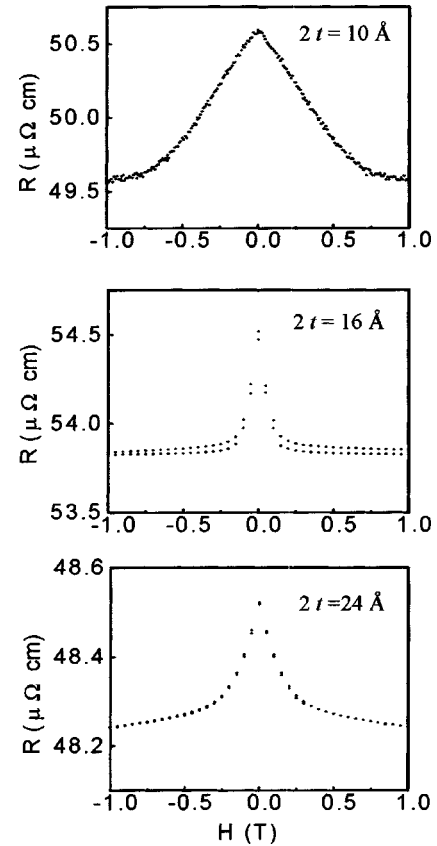


FIG. 4. Magnetoresistance curves at 300 K for $[\text{Fe}(10 \text{ \AA})/\text{Cr}(t \text{ \AA})/\text{Sn}(1 \text{ \AA})/\text{Cr}(t \text{ \AA})]_{\times 39}/\text{Fe}(10 \text{ \AA})$, $2t=10, 16,$ and 24 \AA , grown at 200°C .

the Cr layer thickness increases from 10 to 16 to 24 \AA . This oscillatory behavior of the saturation fields is confirmed also by magnetization measurements. Therefore $\text{Fe}(10 \text{ \AA})/\text{Cr}(t \text{ \AA})/\text{Sn}(1 \text{ \AA})/\text{Cr}(t \text{ \AA})$ multilayers show an oscillatory magnetic coupling consistent with that observed for Fe/Cr multilayers.²⁴ The GMR values are low because the antiferromagnetic coupling between the Fe layers is weakened and the spin-independent electron scattering is increased by the existence of the Sn layers.

C. Mössbauer spectroscopy

The hyperfine fields at the Sn nuclear sites measured by Mössbauer spectroscopy originate mainly from the spin polarization of s electrons at the nuclear sites and can be evaluated from the Fermi-contact term

$$H = (8\pi/3)\mu_B m(0), \quad (1)$$

where, $m(0)$ is the spin density at the nuclear site, μ_B is the Bohr magneton. When the Cr layers in Fe/Cr multilayers are magnetically ordered, the basic spin configuration is thought to be an antiferromagnetic structure with the magnetic moments aligned ferromagnetically in one (001) plane and antiferromagnetically between adjacent (001) planes. The Sn atoms in the present samples are located at substitutional sites of the bcc Cr, which can be paramagnetic or antiferromagnetic. As Sn is a nonmagnetic element, the Sn nuclear

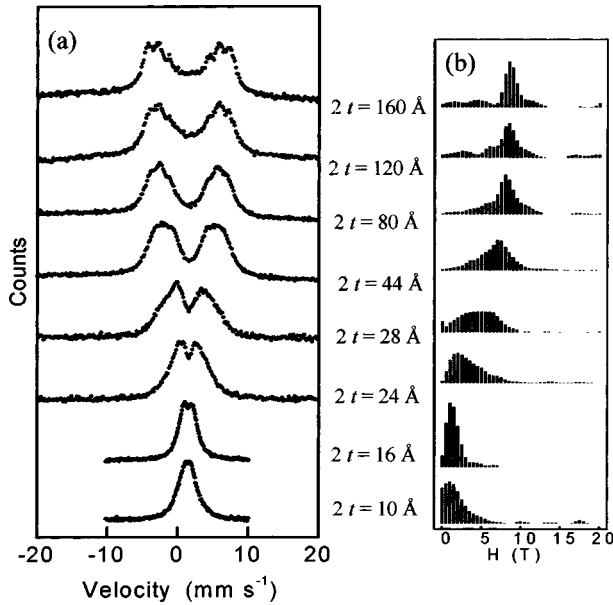


FIG. 5. (a) Mössbauer spectra measured at 300 K for $[\text{Fe}(10 \text{ \AA})/\text{Cr}(1 \text{ \AA})/\text{Sn}(1 \text{ \AA})/\text{Cr}(1 \text{ \AA})]_{\times 39}/\text{Fe}(10 \text{ \AA})$, $2t=10, 16, 24, 28, 4, 80, 120$, and 160 \AA , grown at 200°C and (b) the hyperfine field distribution.

probe can be successfully used to study the magnetic properties of Cr single crystals²⁵ and Cr thin films²¹ by detecting the electron-spin polarization at the Sn nuclear sites, which is induced by the neighboring Cr spin moments.

1. Fe/Cr multilayers grown at elevated temperature

The spectra collected at room temperature for the samples grown at 200°C with the multilayer structures $[\text{Fe}(10 \text{ \AA})/\text{Cr}(t \text{ \AA})/\text{Sn}(1 \text{ \AA})/\text{Cr}(t \text{ \AA})]_{\times 39}/\text{Fe}(10 \text{ \AA})$, where $t_{\text{Cr}}=2t=160, 120, 80, 44, 28, 24, 16$, and 10 \AA , are shown in Fig. 5. Each spectrum was fitted with six Lorentzians 1 mm/s in linewidth, convoluted with a distribution of hyperfine fields. The spectra are symmetric and therefore were fitted assuming that the value of the isomer shift is the same for all the components with different hyperfine fields and that the effect due to the electric quadrupole interaction is negligibly small. The fitted histogram of hyperfine fields was found to have a Gaussian-like distribution. The isomer shift (relative to CaSnO_3) was found to be $1.56 \pm 0.2 \text{ mm/s}$. This is a reasonable value when the Sn atoms are sandwiched by Cr atoms forming a layered structure.²⁶ The Gaussian-like distribution with a relatively sharp distribution width, in comparison with the distribution for dilutely dissolved Sn in a Cr matrix,²⁵ indicates that the magnetic circumstances around the Sn sites are relatively uniform.

The spectrum for Cr layer thickness $2t=80 \text{ \AA}$ shows a clear magnetically split six-line pattern with a distribution of the hyperfine fields. The defined Gaussian-like distribution proves that the Cr magnetic moments are ordered throughout the film with a definite value of the magnetic moment. The main weight in distribution is concentrated between 7 and 12 T with a relative area of about 70% and a peak around 9 T. This large value of the hyperfine field indicates that the mag-

netic moments of the interfacial atomic Cr planes in two antiferromagnetic Cr films, which sandwich the monatomic Sn layer, are oriented to the same direction. In the case when the magnetizations of the interfacial atomic Cr layers sandwiching the Sn layer are antiparallel, a zero net transferred hyperfine field would be expected at the Sn nuclear sites. The intensity ratio of the six peaks in the Mössbauer spectrum shows that the Cr magnetic moments have dominantly in-plane orientation. The best fit gives an average angle of the hyperfine field relative to the film normal of 70° .

When the Cr layer thickness is decreased to $2t=44 \text{ \AA}$, the peak in the hyperfine field shifts to 7 T. A clear reduction of the hyperfine fields is observed by decreasing the Cr layer thickness to 24 \AA . The hyperfine field distribution between 0.5 and 5.5 T has a relative area of 82% and a peak at 2.5 T. By decreasing the Cr layer thickness to 16 \AA , the peak in the distribution is found to be at 2 T and the maximum hyperfine field in the distribution is around 5 T. This defined value of the hyperfine field indicates that the Cr layers still keep the magnetic order throughout the film. For $[\text{Fe}(10 \text{ \AA})/\text{Cr}(5 \text{ \AA})/\text{Sn}(1 \text{ \AA})/\text{Cr}(5 \text{ \AA})]_{\times 39}/\text{Fe}(10 \text{ \AA})$, there is still a distribution of the hyperfine fields up to 5 T with a peak at 1 T.

The Mössbauer spectra measured at low temperatures, down to 15 K, do not show a big temperature dependence.²⁶ Therefore the reduction of the hyperfine fields cannot be attributed to the decrease in the magnetic transition temperature for the smaller Cr layer thickness.

In conclusion, a reduction of the hyperfine fields was observed by decreasing the Cr layer thickness below 80 \AA , while the hyperfine field distributions do not remarkably change by increasing the Cr layer thickness from 80 to 160 \AA . This monotonic reduction of the hyperfine fields is an indication of the gradual reduction of the Cr magnetic moments by decreasing the Cr layer thickness. The reduction of the Cr magnetic moments in Fe/Cr multilayers has been theoretically predicted by tight-binding calculations as a result of the frustrated interlayer magnetic coupling at Fe/Cr rough interfaces.⁵⁻⁷ Due to the strong antiferromagnetic Fe-Cr coupling compared with that of the Cr-Cr coupling, it is energetically less expensive to suppress (or strongly decrease) the Cr magnetic moments near the interfaces than to keep the frustrated magnetic arrangement. Note that the electronic structures of the Fe/Cr/Sn/Cr system with ideally flat interfaces have also been calculated by first-principles calculations,²⁷ where a reduction of the Cr magnetic moments at Cr/Sn interfaces was predicted when Cr layers are sandwiched by Fe layers.

2. Fe/Cr multilayers grown at room temperature

The Mössbauer spectra and the hyperfine field distributions for the multilayer structures of $[\text{Fe}(10 \text{ \AA})/\text{Cr}(t \text{ \AA})/\text{Sn}(1 \text{ \AA})/\text{Cr}(t \text{ \AA})]_{\times 39}/\text{Fe}(10 \text{ \AA})$ ($t_{\text{Cr}}=2t=80, 44, 28$, and 16 \AA) grown at room temperature, are shown in Fig. 6. For the Cr thickness of 80 \AA , the hyperfine fields again have well-defined distribution with about 80% between 9 and 14 T and a peak at 11 T. The comparison of the Mössbauer spectra of samples grown at 200°C and at room temperature shows a clear difference in the intensity ratio of the

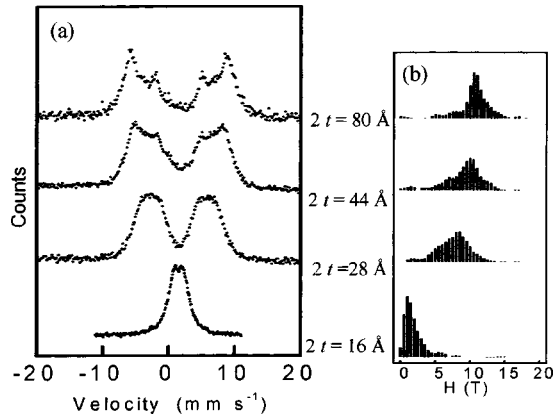


FIG. 6. (a) Mössbauer spectra measured at 300 K for $[\text{Fe}(10 \text{ \AA})/\text{Cr}(t \text{ \AA})/\text{Sn}(1 \text{ \AA})/\text{Cr}(t \text{ \AA})]_{\times 29}/\text{Fe}(10 \text{ \AA})$, $2t=16, 28, 44,$ and 80 \AA grown at room temperature and (b) the hyperfine field distribution.

six split peaks. The spectra collected for the samples grown at room temperature show that the magnetic hyperfine fields tend to orient out of the film plane. The fitted angle of the hyperfine field is 34° relative to the film normal. The hyperfine field distribution for $2t=44 \text{ \AA}$ shows a peak at 10 T with about 80% of the total distribution between 6 and 13 T. By decreasing the Cr layer thickness to 28 \AA , the peak in the distribution shifts to 8 T and the hyperfine field still keeps the out-of-plane orientation. A clear reduction in the hyperfine fields was observed when the Cr layer thickness was reduced to 16 \AA . For this thickness, the Mössbauer spectra are nearly the same for samples grown at 200°C and at room temperature.

The hyperfine fields at the peak in the distribution at different Cr layer thicknesses for the samples grown at 200°C and room temperature are shown in Fig. 7. A clear feature is the larger values of the hyperfine fields observed for Fe/Cr multilayers grown at room temperature in comparison with those grown at high temperatures. We conclude that (i) the Cr magnetic moments tend to orient out of the film plane in Fe/Cr multilayers grown at room temperature and (ii) the Cr magnetic moments are larger when they orient out of the film plane than when they are in the film plane.

The out-of-plane orientation of the Cr magnetic moments indicates that the interlayer Fe-Cr coupling at the interfaces cannot keep the Cr magnetic moments in the film plane.

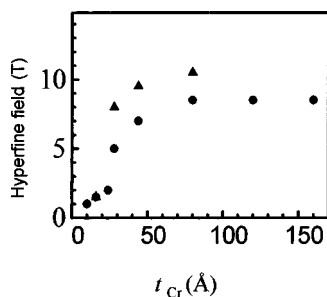


FIG. 7. The hyperfine field at the peak in distribution for samples with different Cr layer thickness grown at 200°C (solid circles) and at room temperature (solid triangles).

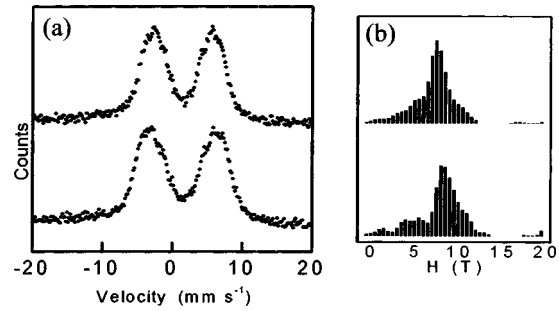


FIG. 8. (a) Mössbauer spectra for $[\text{Fe}(10 \text{ \AA})/\text{Cr}(40 \text{ \AA})/\text{Sn}(1 \text{ \AA})/\text{Cr}(40 \text{ \AA})]_{\times 29}/\text{Fe}(10 \text{ \AA})$ (top) and $[\text{Fe}(10 \text{ \AA})/\text{Cr}(40 \text{ \AA})/\text{Sn}(2 \text{ \AA})/\text{Cr}(40 \text{ \AA})]_{\times 29}/\text{Fe}(10 \text{ \AA})$ (bottom), grown at 200°C and (b) the hyperfine field distribution.

When the Cr magnetic moments rotate away from the in-plane Fe magnetic moments, the frustration of the magnetic coupling energy among the Fe-Cr pairs would decrease. Therefore the out-of-plane orientation of the Cr magnetic moments is another way through which the Cr magnetic moments can escape from the magnetic frustration at rough interfaces. It is plausible that the reduction of the Cr magnetic moments observed for samples grown at elevated temperatures results from the magnetic frustration among the in-plane oriented Cr and Fe magnetic moments. In the case when the Cr magnetic moments orient out of the film plane, the magnetic frustration energy would be smaller and the Cr magnetic moments are expected to be kept large. The smaller lateral length scale of interface steps, expected for Fe/Cr multilayers grown at room temperature than at elevated temperatures,¹⁷ is thought to be the origin of the reorientation of the Cr magnetic moments. The orientation of the Cr magnetic moments perpendicular to the in-plane Fe magnetic moments in Fe/Cr multilayers was also observed by neutron diffraction.¹³

3. Samples with different probe layer thickness

To confirm that the Fe/Cr interface conditions play the main role of controlling the magnetic structure of Cr layers in Fe/Cr/Sn/Cr multilayers, samples with 1 and 2 \AA of the Sn layer have been grown at 200°C . As shown in Fig. 8 for the sample with the Cr layer thickness of 80 \AA , neither the magnitude nor the orientation of the hyperfine field is affected much by increasing the Sn probe layer thickness, in contrast with the remarkable dependence on the growth temperature. Therefore, the observed dependence of the Mössbauer spectra on the growth temperature can be attributed to the change in frustration effect at the Fe/Cr interfaces rather than that at the Cr/Sn interfaces. The conduction-electron polarization mediates the spin configuration of Cr across the Sn layer without causing magnetic frustration at the Cr/Sn interfaces. (Note that the relative ratio of the components with smaller hyperfine fields increases when the Sn layer thickness increases more, since the effective number of Sn atoms which do not contact Cr atoms, and hence with a smaller s -electron spin polarization, becomes larger.) The role of the Fe/Cr interface is also confirmed by the Mössbauer results of V/Cr multilayers with Sn (2 \AA) probe layers in the Cr layers,

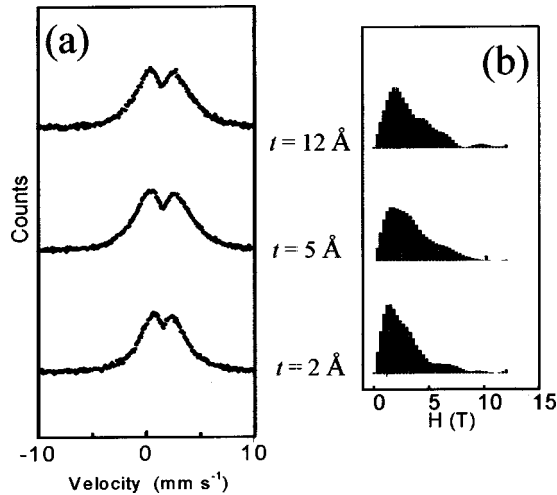


FIG. 9. (a) Mössbauer spectra measured at 300 K for $[\text{Fe} (10 \text{ \AA})/\text{Cr} ([24-t] \text{ \AA})/\text{Sn} (2 \text{ \AA})/\text{Cr} (t \text{ \AA})]_{\times 39}/\text{Fe} (10 \text{ \AA})$, $t = 2, 5, \text{ and } 12 \text{ \AA}$, grown at 200°C and (b) the hyperfine field distribution.

where magnetic frustration is not expected at the V/Cr interfaces. The spectra for this system show nearly the same feature for the samples grown at both room temperature and 200°C , independent of the growth temperature.²⁸

4. Local magnetic structure of Cr as a function of the depth from Fe interface

The local magnetic structures along the direction perpendicular to the film plane were characterized by inserting the Sn probe at different distances from the Fe/Cr interface for a fixed Cr layer thickness.

The Mössbauer spectra and the hyperfine field distributions for Sn sites at 2, 5, and 12 Å from the Fe interface for Fe/Cr multilayers with Cr layer thickness of 24 Å are shown in Fig. 9. The hyperfine field distributions are nearly the same for the three samples having a peak at 2 T. A little increase of the relative ratio in the region from 2 to 6 T was observed as the Sn submonolayer goes to the center of the Cr layers. Therefore the Cr layers have an ordered magnetic structure with a reduced magnetic moment, and the local magnetic structure of Cr around Sn does not change throughout the Cr layers.

For the Cr layers with the thickness of 160 Å, the hyperfine field distribution shows a peak at 8 T when the Sn layer is located at the center of the Cr layers (i.e., at a distance of 80 Å from the Fe interface) as shown in Fig. 10. When the Sn probe is located at 5 Å from the Fe interface, the peak in the distribution is at 7.5 T. The ratio of the fitted six lines of the magnetically splitted spectra indicates that the hyperfine field is dominantly oriented in the film plane. The observed decrease in the second and fifth lines relative to the first and sixth lines, as the Sn position goes toward the middle of the Cr layer, indicates the tendency of the spins to rotate out of the film plane as the position goes away from Fe interfaces.

Note that the Mössbauer studies for V/Cr/Sn/Cr multilayers show a clear reduction of the hyperfine fields as the Sn monolayers are located nearer to the V/Cr interfaces.²⁸ In

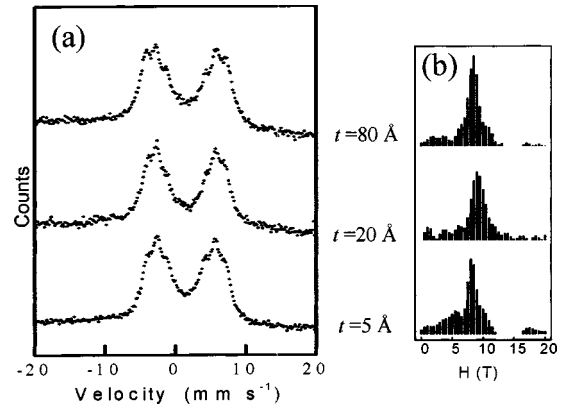


FIG. 10. (a) Mössbauer spectra measured at 300 K for $[\text{Fe} (10 \text{ \AA})/\text{Cr} ([160-t] \text{ \AA})/\text{Sn} (2 \text{ \AA})/\text{Cr} (t \text{ \AA})]_{\times 24}/\text{Fe} (10 \text{ \AA})$, $t = 5, 20, \text{ and } 80 \text{ \AA}$, grown at 200°C and (b) the hyperfine field distribution.

these multilayers, the V layers reduce the magnetic moment of Cr strongly near the V/Cr interfaces. Also the depth profile of the present system shows a different feature from that of magnetic/nonmagnetic multilayers such as Fe/Ag and Co/Au multilayers with ^{119}Sn probe layers.²⁹ In these multilayers, the influence of the Fe layers was reported to increase strongly toward the Fe/nonmagnetic interface. The induced spin polarization of the spacer conduction electrons by the ferromagnetic Fe layer is the origin of the observed hyperfine fields in the nonmagnetic element. In Fe/Cr multilayers, the hyperfine fields at ^{119}Sn nuclear sites were found to change as a function of the total Cr layer thickness between the Fe layers rather than as a function of the distance from the Fe/Cr interfaces. This confirms that a long-range order exists in the Cr layers, with the size of the magnetic moment depending on the Cr layer thickness in the whole thickness range studied. These results are consistent with the magnetic phase diagram for Fe/Cr multilayers obtained by neutron-diffraction measurements, which refers to a CSDW in the Cr layers at room temperature, with the Cr magnetic moments oriented in the film plane.^{13,14}

IV. CONCLUSIONS

Fe/Cr multilayers grown at elevated temperatures show a preferred in-plane orientation of the Cr magnetic moments. A gradual reduction of the Cr magnetic moments was observed as the Cr layer thickness decreases, and can be explained by the competition between the interface frustration, which tends to reduce the Cr magnetic moments, and the Cr-Cr antiferromagnetic coupling, which tends to keep the magnitude of the magnetic moment. For Fe/Cr multilayers grown at room temperature, the interface coupling appears to be smaller and the Cr magnetic moments break the antiferromagnetic alignment at the Fe/Cr interface and rotate out of the film plane. In this case, the interface magnetic frustration can be relieved by the reorientation of the Cr magnetic moments away from the in-plane Fe magnetic moments and therefore the Cr layers can have larger magnetic moments.

ACKNOWLEDGMENTS

The authors thank Dr. N. Hosoi, Dr. T. Oguchi, and Dr. K. Hirai for fruitful discussions during this work. This work

was partially supported by Grants-in-Aid for Research for the Future from the Japan Society for the Promotion of Science and COE Research from the Ministry of Education, Science, Sports and Culture.

*Present address: Physics Department, Assiut University, Egypt.

¹H. Zabel, *J. Phys.: Condens. Matter* **11**, 9303 (1999).

²T. D. Pierce, J. Unguris, R. J. Celotta, and M. D. Stiles, *J. Magn. Magn. Mater.* **200**, 290 (1999).

³E. Fawcett, *Rev. Mod. Phys.* **60**, 209 (1988).

⁴A. Berger and E. E. Fullerton, *J. Magn. Magn. Mater.* **165**, 471 (1997).

⁵D. Stoeffler and F. Gautier, *J. Magn. Magn. Mater.* **147**, 260 (1995).

⁶D. Stoeffler and F. Gautier, *Phys. Rev. B* **44**, 10 389 (1991).

⁷D. Stoeffler and F. Gautier, *J. Magn. Magn. Mater.* **121**, 259 (1993).

⁸R. S. Fishman, *Phys. Rev. Lett.* **81**, 4979 (1998).

⁹R. S. Fishman and Zhu-Pei Shi, *Phys. Rev. B* **59**, 13 849 (1999).

¹⁰J. C. Slonczewski, *J. Magn. Magn. Mater.* **150**, 13 (1995).

¹¹E. E. Fullerton, S. D. Bader, and J. L. Robertson, *Phys. Rev. Lett.* **77**, 1382 (1996).

¹²E. E. Fullerton, K. T. Riggs, C. H. Sowers, S. D. Bader, and A. Berger, *Phys. Rev. Lett.* **75**, 330 (1995).

¹³P. Bödeker, A. Schreyer, and H. Zabel, *Phys. Rev. B* **59**, 9408 (1999).

¹⁴A. Schreyer, C. F. Majkrzak, Th. Zeidler, T. Schmitte, P. Bodeker, K. Theis-Bröhl, A. Abromeit, J. A. Dura, and T. Watanabe, *Phys. Rev. B* **79**, 4914 (1997).

¹⁵J. F. Ankner, H. Kaiser, A. Schreyer, T. Zeidler, H. Zabel, M. Schäfer, and P. Grünberg, *J. Appl. Phys.* **81**, 3765 (1997).

¹⁶E. E. Fullerton, S. D. Bader, and J. L. Robertson, *Phys. Rev. Lett.* **77**, 1382 (1996).

¹⁷A. Schreyer, J. F. Ankner, T. Zeidler, H. Zabel, M. Schäfer, J. A. Wolf, P. Grünberg, and C. F. Majkrzak, *Phys. Rev. B* **52**, 16 066 (1995).

¹⁸T. Schmitte, A. Schreyer, V. Leiner, R. Siebrecht, K. Theis-Bröhl, and H. Zabel, *Europhys. Lett.* **48**, 692 (1999).

¹⁹J. Meersschant, J. Dekoster, R. Scad, and M. Rots, *Phys. Rev. Lett.* **75**, 1638 (1995).

²⁰J. Meersschant, J. Dekoster, S. Demuynck, S. Cottenier, B. Swinnen, and M. Rots, *Phys. Rev. B* **57**, R5575 (1998).

²¹K. Mibu, S. Tanaka, and T. Shinjo, *J. Phys. Soc. Jpn.* **67**, 2633 (1998).

²²J. A. Stroschio, D. T. Pierce, and R. A. Dragoset, *Phys. Rev. Lett.* **70**, 3615 (1993).

²³K. Ishiji, H. Okuda, H. Hashizume, M. Almokhtar, and N. Hosoi, *Phys. Rev. B* **66**, 014443 (2002).

²⁴S. S. P. Parkin, N. More, and K. P. Roche, *Phys. Rev. Lett.* **64**, 2304 (1990).

²⁵S. M. Dubiel, J. Cieślak, and F. E. Wagner, *Phys. Rev. B* **53**, 268 (1996).

²⁶K. Mibu, M. Almokhtar, S. Tanaka, A. Nakanishi, T. Kobayashi, and T. Shinjo, *Phys. Rev. Lett.* **84**, 2243 (2000).

²⁷H. Momida and T. Oguchi, *J. Magn. Magn. Mater.* **234**, 126 (2001).

²⁸M. Almokhtar, K. Mibu, A. Nakanishi, T. Kobayashi, and T. Shinjo, *J. Phys.: Condens. Matter* **12**, 9247 (2000).

²⁹T. Emoto, N. Hosoi, and T. Shinjo, *J. Phys. Soc. Jpn.* **66**, 803 (1997).